Journal of Nuclear Medicine, published on September 22, 2016 as doi:10.2967/jnumed.116.179648

CT radiomic analysis using lymph-node-density profile in correlation to SUV-value for PET/CT based N-Staging

Frederik L. Giesel[1,2]; Florian Schneider[1]; Clemens Kratochwil[1]; Daniel Rath[1]; Jan Moltz[3]; Tim Holland-Letz[4]; Hans-Ulrich Kauczor[5,6]; Lawrence H. Schwartz[7]; Uwe Haberkorn[1,2,6]; Paul Flechsig[1,5,6]

1) University Hospital Heidelberg, Department of Nuclear Medicine, Heidelberg, Germany
2) Clinical Cooperation Unit, Department of Nuclear Medicine, DKFZ, Heidelberg, Germany
3) Fraunhofer MEVIS, Institute for Medical Image Computing, Bremen, Germany
4) Department of Biostatistics, German Cancer Research Center, Heidelberg, Germany
5) University Hospital Heidelberg, Department of Diagnostic and Interventional Radiology; Heidelberg, Germany
6) Translational Lung Research Center Heidelberg, Member of the German Center for Lung Research DZL; Heidelberg, Germany
7) Columbia University Medical Centre, New York Presbyterian Hospital, Department of Radiology, New York, USA New York Presbyterian Hospital

Corresponding Author:
Paul Flechsig
Department of Nuclear Medicine, University Hospital Heidelberg
INF 400
69120 Heidelberg
Phone: +49-6221-56-7733
e-mail: paul.flechsig@med.uni-heidelberg.de

First Author:
Frederik L. Giesel
Department of Nuclear Medicine, University Hospital Heidelberg
INF 400
69120 Heidelberg
Phone: +49-6221-56-39461
e-mail: frederik@egiesel.com

Word count:
5000

Short running title:
CT-density in PET-based N-staging

ABSTRACT

In patients with lung cancer (LC), malignant melanoma (MM), gastroenteropancreatic neuroendocrine tumours (GEP-NETs) and prostate cancer (PCA), N-staging is often performed by integrated ^{18}F-FDG-Positron Emission Tomography/Computed Tomography (PET/CT) (LC, MM), ^{68}Ga-DOTATOC-PET/CT (GEP-NET) and ^{68}Ga-PSMA-PET/CT (PCA): N-staging is not always accurate due to indeterminate PET-findings. To better evaluate malignant lymph node (LN) infiltration, additional surrogate parameters, especially in cases with indeterminate PET-findings, would be helpful. The purpose of this study was to evaluate if maximal standardized uptake values (SUVmax) in the PET-examination might correlate with semi-automated density measurements of LN in the CT-component of the integrated PET/CT examination.

Methods: After approval by the institutional review board, 1022 LNs in PET/CT-examinations of 148 patients were retrospectively analysed (LC: 327 LN out of 40 patients, MM: 224 LN out of 33 patients; GEP-NET: 217 LN out of 35 patients, PCA: 254 LN out of 40 patients). PET/CT was performed before surgery/biopsy, chemotherapy, or internal or external radiation therapy, according to the clinical schedule, patients with prior chemotherapy or radiation therapy were ruled out. LN analyses were performed on the basis of SUV-uptake 60 minutes after tracer injection and volumetric CT histogram analysis in non-contrast enhanced CT.

Results: LNs were considered positive or negative on the basis of tracer uptake, histological confirmation was not available. Of the 1022 lymph nodes, 331 had positive SUVmax-findings (3-times SUVmax of bloodpool), 86 were indeterminate (1-3 SUVmax bloodpool), 605 were negative (< SUVmax bloodpool). LNs with positive SUV-uptake had significantly higher CT-density values compared to PET-negative LN, irrespective of the cancer entity.

Conclusion: Density measurements of LNs in patients with LC, MM, GEP-NET and PCA correlate with FDG uptake in PET, and might therefore serve as an additional surrogate parameter for the differentiation between malignant and benign LNs. A possible density threshold in clinical routine might be a 7.5 Hounsfield Units (HU) cut-off value to differentiate

between malignant and benign LN infiltration, and a 20 HU cut off to exlude benign lymph node processes, especially helpful in PET-indeterminate LNs.

Key words:

N-staging, FDG-PET-CT, DOTATOC-PET/CT, PSMA-PET/CT, radiomics

INTRODUCTION

One of the most widespread and reliable non-invasive staging tools for cancer patients is PET/CT, namely ^{18}F-FDG-PET/CT for patients with lung cancer (LC, (*1*,*2*)) and malignant melanoma (MM, (*1*,*3*)), ^{68}Ga-PSMA-PET/CT for patients with prostate cancer (PCA, (*4*)), and ^{68}Ga-DOTATOC-PET/CT for patients with gastroenteropancreatic neuroendocrine tumours (GEP-NET, (*5*)). An exact evaluation of LN-status prior to therapy is crucial for therapy planning. False positive PET-findings are not uncommon with FDG-PET/CT, since the scan can mistakenly pick up on inflammation due to infectious etiologies e.g. of the lung or the head and neck area (*3*,*6*). Therefore, invasive LN-staging is mandated in different guidelines to verify PET-positive lymph nodes, especially in cases of a curative therapy approach (*7*), not only in patients with FDG-PET/CT. In order to further develop imaging biomarkers and to capture intra-tumoural heterogeneity non-invasively, we employed techniques used in the rapidly evolving field of radiomics (*8*).

To examine possible correlations between the functional PET-, and the morphological CT-component of integrated PET/CT, metric and functional parameters including volumetric histogram analysis, lymph node density, and SUVmax were evaluated in lymph nodes of patients with LC, MM, GEP-NET and PC. For lung cancer patients, increased lymph node densities have been reported in metastatic lymph nodes in two different studies with cohorts of 45 (*6*) and 72 patients (*9*). For patients with MM, GEP-NET and PCA, no data with correlations between histological lymph node status, SUVmax and CT-density are currently available.

We hypothesized that in LN-metastases of the above mentioned tumour entities, positive correlations between tracer accumulation, as a functional measure for malignant lymph node infiltration, and CT densities, as a possible metric surrogate parameter for LN-infiltration, might be evident. Therefore, lymph node density was defined as the primary endpoint, and short-axis diameter (SAD) and SUV were regarded as secondary endpoints.

MATERIALS AND METHODS

Study design and Patients

The study was conducted in the setting of a single centre design. Lymph node density and (SAD) of the assessed lymph nodes were examined in non-contrast CT using dedicated analysis software for semi-automated lymph node segmentation ((*6*)). A total of 1024 lymph nodes in 148 patients (86 male, median age 62 years) were examined (LC: 327 LN out of 40 patients; MM: 224 LN out of 33 patients; GEP-NET: 217 LN out of 35 patients; PCA: 254 LN out of 40 patients). All PET/CT-examinations were performed according to the clinical schedule prior to surgical resection, chemotherapy or radiation therapy. The study was approved by the institutional review board and conducted according to the guidelines of the institutional review board and to good clinical practice according to the ethical principles that have their origin in the Declaration of Helsinki. In this retrospective analysis, the requirement of informed consent was waived by the institutional review board.

PET/CT-examinations

All PET/CT-examinations were performed for staging and therapeutic planning according to the clinical routine using a Biograph 6 PET/CT-Scanner (Siemens Medical Solution, Knoxville, USA) with the following examination protocols and reconstruction parameters: slice thickness/reconstruction increment of 5.0/2.5mm, standard soft-tissue reconstruction kernel B30. Patients, who had undergone neoadjuvant radiation and / or chemotherapy prior to the PET/CT-examination, were ruled out.

Static emission scans (eight bed positions, 4 min each) were acquired from the vertex to the proximal legs with correction for dead time, scatter and decay. For attenuation correction, non-enhanced low dose CT was used (*10*). Emission scan images were iteratively reconstructed using ordered subset expectation maximisation algorithm (four iterations, eight subsets and Gaussian filtering), resulting in an in-plane spatial resolution of 5mm at full-width half-maximum (*10,11*). CT analyses were performed on the basis of native CT scans accompanying each of the integrated PET/CT examinations. FDG-uptake, DOTATOC-uptake and PSMA-

uptake were evaluated using the parameter SUV_{max}. Due to internal clinical standards for the evaluation of LNs in FDG-PET/CT examinations in our department, PET-findings were a priori classified as PET-positive, when SUVmax in the assessed LN ≥ 3-times SUVmax bloodpool, PET-indeterminate when SUVmax (LN) = 1-3-times SUVmax bloodpool, PET-negative when SUVmax (LN) ≤ SUVmax bloodpool, irrespective of tumour type and tracer.

Radionuclide-administration, PET-acquisition and PET-interpretation

^{18}F-FDG-PET. After fasting for at least 8h (blood glucose level below 150mg/dl), 4MBq/kg body weight of ^{18}F-fluordesoxyglucose (FDG) were administered intravenously 60 ± 5 minutes before the FDG-PET/CT scan.

^{68}Ga-DOTATOC-PET/CT. DOTA(0)-Phe(1)-Tyr(3)-octreotide (DOTATOC)-PET-imaging started 60 ± 5 minutes after intravenous injection of 80-200 MBq of ^{68}Ga-DOTATOC.

^{68}Ga-PSMA-PET. ^{68}Ga-prostate-specific membrane antigen (PSMA) ligand positron emission tomography (PET)-imaging was performed 60 ± 5 minutes post-injection (p.i.) of 150-250 MBq of ^{68}Ga-PSMA.

Volumetric CT histogram analyses

Morphological LN-assessment and volumetric CT histogram analysis was performed by a radiologist with 5 years of experience in oncologic imaging, blinded to clinical information. Volumetric LN-analysis was performed semi-automatically (Fraunhofer MEVIS, Bremen, Germany (*12*)). Metric analyses and histogram analyses were initiated by providing a seed point in the investigated lymph node. Within an estimated region of interest, thresholds were generated automatically by the segmentation software with a high level of reproducibility of the semi-automated segmentation process alone of ≥ 90% (*6*). In a next step spatial parameters were extracted and histogram analysis was performed automatically by the software (*6*). For validation reasons, results from semi-automated lymph node evaluation were verified by the conducting physician, who visually went through all three dimensions of each of the assessed lymph nodes using the integrated 3D viewer for multiplanar reconstruction (*6*). If necessary, semi-automated segmentations was corrected manually in all three dimensions.

Statistical Analysis

Statistical analysis was performed using SigmaPlot (Systat Software GmbH, Erkrath). Median values for density, SAD, and SUV_{max} with 95% confidence interval were calculated and illustrated in Box-Whisker-Plots. Differences were considered significant at $p < 0.05$ in a two sided paired sample t test for the calculation of SAD and density, and a two sided Wilcoxon Signed Rank Test for the calculation of SUV_{max}. Diagnostic accuracy of all four variables was investigated using Receiver Operating Characteristic (ROC)-analysis.

RESULTS

PET-findings

Among the different tumour entities, number (n) of PET-positive (PET+), PET-indeterminate (PET +/-), and PET-negative (PET-) LN was distributed as mentioned in *Table 1, Fig. 1*. Except for the population of patients with GEP-NET's, where SUV_{max} was either below the mediastinal bloodpool, or more than triple than bloodpool, PET-positive, PET-indeterminate- and PET-negative LN were found for all tumour entities.

Metric and functional LN analysis

For semi-automated LN analysis, less than 1 minute of additional reading time was necessary for the evaluation of each lymph node, including semi-automated size-, and density measurements.

LC-patients. LN-density was significantly higher in PET+ LN (31.3HU) compared to PET- LN (-12,6 HU; p<0.01, Table 1, Fig. 2A), which was correlating well with the corresponding LN-histograms of averaged PET+, PET +/- and PET- LN (Fig. 2B). SAD was significantly higher in PET+ LN (12.7mm) compared to PET+/- (7.8mm; p<0.01) and PET- LN (5.7mm; p<0.01, Table 1, Fig. 2C).

MM-patients. LN-density was significantly higher in PET+ LN (27.9HU) compared to PET- LN (-16.3HU; p<0.01, Table 1, Fig. 3A), which was correlating well with the corresponding LN-histograms of averaged PET+, PET +/- and PET- LN (Fig. 3B). SAD was significantly

higher in PET+ LN (10mm) compared to PET+/- (8.3mm; $p<0.05$) and PET- LN (5mm; $p<0.01$, Table 1, Fig. 3C).

GEP-NET-patients. Since there were no findings of PET-indeterminate LN, it was only possible to correlate PET+ and PET- LN. LN-density was significantly higher in PET+ LN (33.7HU) compared to PET- (-11.6HU; $p<0.01$, Table 1, Fig. 4A). This was also evident in the corresponding LN-histograms of averaged PET+ and PET- LN (Fig. 4B). SAD of PET+ LN (9.7mm) was significantly higher compared to PET- LN (5.6mm; $p<0.01$, Table 1, Fig. 4C).

PCA-patients. LN-density was significantly higher in PET+ LN (19.2HU) compared to PET- LN (-23.7HU; $p<0.01$, Table 1, Fig. 5A). There was no significant difference of LN-density between PET+ (19.2HU) and PET+/- LN (9.9HU; $p = 0.06$, Table 1), nevertheless PET+/- LN tended to have a lower density compared to PET+ LN. LN-density between PET+/- and PET- LN is significantly different ($p<0.01$; Table 1). Corresponding LN-histograms of averaged PET+, PET +/- and PET- LN are shown in Fig. 5B. SAD was significantly higher in PET+ LN (7.1mm) compared to PET- LN (5.5mm; $p<0.01$), but there was no statistically significant difference between PET+ and PET+/- LN in concerns of LN SAD ($p=0.78$, Table 1, Fig. 5C), as well as between PET+/- and PET- LN ($p=0.21$, Table 1, Fig. 5C).

Density-based cut of value

In patients with LC, 96% of PET+ LNs presented with a LN-density >7.5HU, while 91% of PET- LNs presented with LN-density values < 7.5HU (Fig. 2A). Density of all PET- LNs was < 20HU (Table 1).

Regarding MM-patients, 91% of PET+ LNs presented with a LN-density >7.5HU, while 90% of PET- LNs presented with LN-density values < 7.5HU (Fig. 3A). LN-density of 99% of PET- LNs was < 20HU (Table 1).

In patients with GEP-NET, 96% of PET+ LNs presented with a LN-density >7.5HU, while 89% of PET- LNs presented with LN-density values < 7.5HU (Fig. 4A). Density of all PET- LNs was < 20HU (Table 1).

Regarding LNs in PCA-patients, 77% of PET+ LNs presented with a LN-density >7.5HU, while 96% of PET- LNs presented with LN-density values < 7.5HU (Fig. 5A). Density of 99% of PET- LNs was < 20HU (Table 1).

Regarding all LNs irrespective of tumour entity, 89% of PET+ LNs presented with a LN-density >7.5HU, while > 92% of PET- LNs presented with LN-density values < 7.5HU (Fig. 6). Density of > 99% of PET- LNs was < 20HU (Fig. 6). Regarding the cohort of PET +/- LNs, nearly one halve of the LNs presents with CT-densities < 20HU (43%), 83% present with CT-densities >7.5HU (Fig. 6).

ROC analyses and Area Under the Curve (AUC)

Regarding ROC-analyses, higher values for AUC were calculated for LN-density as compared to LN SAD for all tumour entities, using PET-positivity as standard of reference (AUC-values (LN-density vs. LN-SAD): LC 0.99 vs. 0.93 (Supplemental Fig. 2D); MM 0.97 vs 0.89 (Supplemental Fig. 3D); GEP-NET 0.98 vs 0.85 (Supplemental Fig. 4D); PCA 0.92 vs 0.7 (Supplemental Fig. 5D)), indicating a higher correlation between the parameters PET and LN-density compared to PET and SAD.

DISCUSSION

We found significantly higher CT-density values in PET+ LNs in patients with LC, MM, GEP-NET and PCA compared to PET- LNs by means of semi-automated, CT histogram analysis. In FDG-PET/CT examinations of patients with MM, we also found significantly higher density values in PET+ LNs compared to PET+/- LNs. Regarding ROC-analyses with PET-positivity as standard of reference, we found higher AUC-values for the parameter CT-density as compared to the metric parameter SAD, which is commonly used in Response Evaluation Criteria In Solid Tumors 1.1 measurements. Based on the hypothesis that PET-positivity is a measure for malignant LN-infiltration in the above mentioned tumour entities, which needs to be confirmed and validated in an independent cohort of patients, a possible cut-off value of 7.5HU might serve as an additional surrogate parameter for the differentiation between malignant and benign LN involvement in patients with LC, MM; GEP-NET and PCA.

In the cohort of 1022 LNs, irrespective of tumour entity, 89% of PET+ LNs presented with density-values above the 7.5HU cut off, while 92% of PET- LNs presented with LN-density values below the 7.5HU cut off value. Thus, a possible cut off value of 7.5HU might help to further discriminate between benign and malignant LN infiltration, which is of clinical relevance, especially in the cohort of PET +/- LNs with 83% of LNs presenting with CT-density values above the 7.5HU cut off.

Another cut off value, that can possibly help to exclude benign lymph nodes is the 20HU cut off with >99% of the benign LNs being below the 20HU cut off, indicating that LNs with CT-density values >20HU are most likely to be of malignant histology. This is of outstanding clinical interest, since an exact LN-classification plays an integral role in diagnostic tumour staging, therapy stratification and post-surgical follow-up imaging.

The fact, that PET-positivity is a clinically valuable measure for malignant LN-infiltration has been demonstrated with a sensitivity of 89%, specificity of 84%, and a negative predictive value of 96% in patients with LC (*13*). The use of PET/CT for staging and follow-up examinations in patients with MM was proven in several studies with a sensitivity of 96%, specificity of 92%, a positive predictive value for the 92% and a negative predictive value of 95% for the relapse of neoplasm in a recently published systemic review (*14*). Regarding patients with SSTR-positive GEP-NETs, the excellent clinical use of DOTATOC-PET/CT for the detection of primary tumours, LN metastases and distant metastases could be demonstrated in several studies, as well as the potential of SSTR-based therapies (*15*). In patients with PCA, a recently published study demonstrated a sensitivity of 86.9%, specificity of 93.1%, a positive predictive value of 75.7% and a NPV of 96.6% for LN-staging in patients observed by ^{68}Ga-PSMA-PET/CT (*4*).

A possible density cut off value for N-staging focusing on patients with LC, with histopathological correlate as standard of reference, has been proposed earlier (*6*) proposing a cut off value of 20HU. Other groups have found strong correlations between LN-density, SUV_{max}-ratios and malignant LN infiltration in patients with NSCLC without mentioning a dedicated, density-based cut off value feasible for clinical routine (*9*). Recently published data from an animal study showed possible, density-based cut off values for the differentiation

between malignant and benign LNs in animals without mentioning a possible cut off value which might be applied in humans (*16*).

In patients with LC, the high diagnostic accuracy of integrated ^{18}F-FDG-PET/CT in terms of lymph node staging revealed a high diagnostic accuracy *(13,17-22)*, with exceptions for very small LNs that need invasive intrathoracic LN sampling *(23)*. In clinical routine, combined analysis of the metric parameter SAD, according to Response Evaluation Critieria In Solid Tumours 1.1, and the functional parameter SUV_{max} allows for most reliable non-invasive staging, usually performed using integrated ^{18}F-FDG-PET/CT *(24-26)*. According to McIvor et al., ^{18}F-FDG-PET/CT could help to detect unsuspected sites of MMs in 17% of early stage MM, where integrated ^{18}F-FDG-PET/CT is usually not performed, as recommended in established guidelines *(27)*. In patients with PCA, according to Zattoni et al.(*28*), pre-therapeutic ^{68}Ga-PSMA-PET/CT can help to find possible high yield targets for salvage lymph node dissections, but the authors still state the need for novel biomarkers in order to further improve clinical output.

The use of LN-density as a possible surrogate parameter for malignant LN-infiltration has been discussed in a recently published study focusing on patients with breast cancer (*29*). In the above mentioned study, x-ray phase contrast Micro-Tomography was used in a preclinical trial for density evaluation of LNs. The authors of this study reported that x-ray phase contrast Micro-Tomography revealed a high potential for non-invasive lymph node staging for the assessment of loco regional LNs in the axilla. In tumours besides the above mentioned entities, the use of metric surrogate parameters could be demonstrated for patients with malignant lymphomas. In a retrospectively performed study, volumetric lymph node analysis significantly improved lesion classification compared to the commonly used parameter long-axis diameter *(30)*.

The potential for functional PET-parameters that could serve as surrogate parameters for TNM-staging in oncologic imaging have been demonstrated in a variety of recently published data. According to Cerfolio et al., primary tumours of LC patients in higher tumour stages present with higher SUV_{max} values compared to patients with lower tumour stages in ^{18}F-FDG-PET/CT-examinations. Cuaron et al. found out that FDG-uptake of the primary tumours varies

between different tumour entities in LC patients *(31)*, which might be due to differences in the expression of glucose transporters, according to Brown et al. *(32)*.

Due to uncertainties in non-invasive PET/CT-based oncologic imaging, invasive staging techniques, such as core cut biopsies of the primary tumour, possible LN metastases or distant metastases are often mandatory in clinical routine. In these cases, additional information derived from density-based semi-automated LN-analysis might potentially lead to high yield targets for invasive staging, especially when information on functional PET-parameters (e.g. SUV_{max}) and metric CT parameters (e.g. SAD) are used in combination. In the long term, the use of additional surrogate parameters such as density-based cut off values for LN-analyses might not only help to find high-yield targets for biopsies, but could possibly lead to a reduced need for invasive staging procedures due to better prognostic predictability of TNM-stages in non-invasive PET/CT-imaging. Density-based cut-off values as possible imaging biomarkers might potentially be generated automatically in clinical routine in the future, thus helping to further categorize unclear imaging findings as part of the recently evolving field of radiomics (*8*).

A limitation of this study is the retrospective design, and the lack of histopathological correlations for the PET- and CT-findings. In order to clearly define dedicated CT-density cut off values to malignant and benign LNs, it might be helpful to perform prospective studies for all the above mentioned tumour entities, focusing of the analysis of preoperative PET/CT-examinations, which would then be correlated with histopathological findings. Nevertheless, a restriction to preoperative patients would lead to a focus on patients with lower tumour stages.

CONCLUSION

Semi-automated CT-density analysis of LNs in patients with LC, MM, GEP-NET and PCA could possibly be used as a valuable surrogate parameter in order to improve N-staging in integrated PET/CT, using 7.5HU as a possible cut off value for the discrimination of malignant and benign LNs, and a 20HU cut off to exclude LN benignancy.

DISCLOSURE

There is no potential conflict of interest relevant to this article.

REFERENCES

1. Petersen H, Holdgaard PC, Madsen PH, et al. FDG PET/CT in cancer: comparison of actual use with literature-based recommendations. *Eur J Nucl Med Mol Imaging.* 2016;43:695-706.

2. Kratochwil C, Haberkorn U, Giesel FL. [PET/CT for diagnostics and therapy stratification of lung cancer]. *Radiologe.* 2010;50:684-691.

3. Pfluger T, Melzer HI, Schneider V, et al. PET/CT in malignant melanoma: contrast-enhanced CT versus plain low-dose CT. *Eur J Nucl Med Mol Imaging.* 2011;38:822-831.

4. Pfister D, Porres D, Heidenreich A, et al. Detection of recurrent prostate cancer lesions before salvage lymphadenectomy is more accurate with Ga-PSMA-HBED-CC than with F-Fluoroethylcholine PET/CT. *Eur J Nucl Med Mol Imaging.* 2016.

5. Maxwell JE, Howe JR. Imaging in neuroendocrine tumors: an update for the clinician. *Int J Endocr Oncol.* 2015;2:159-168.

6. Flechsig P, Kratochwil C, Schwartz LH, et al. Quantitative volumetric CT-histogram analysis in N-staging of 18F-FDG-equivocal patients with lung cancer. *J Nucl Med.* 2014;55:559-564.

7. Goeckenjan G, Sitter H, Thomas M, et al. [Prevention, diagnosis, therapy, and follow-up of lung cancer. Interdisciplinary guideline of the German Respiratory Society and the German Cancer Society--abridged version]. *Pneumologie.* 2011;65:e51-75.

8. Lambin P, Rios-Velazquez E, Leijenaar R, et al. Radiomics: extracting more information from medical images using advanced feature analysis. *Eur J Cancer.* 2012;48:441-446.

9. Shao T, Yu L, Li Y, Chen M. [Density and SUV ratios from PET/CT in the detection of mediastinal lymph node metastasis in non-small cell lung cancer]. *Zhongguo Fei Ai Za Zhi.* 2015;18:155-160.

10. Flechsig P, Zechmann CM, Schreiweis J, et al. Qualitative and quantitative image analysis of CT and MR imaging in patients with neuroendocrine liver metastases in comparison to (68)Ga-DOTATOC PET. *Eur J Radiol.* 2015;84:1593-1600.

11. Giesel FL, Kratochwil C, Mehndiratta A, et al. Comparison of neuroendocrine tumor detection and characterization using DOTATOC-PET in correlation with contrast enhanced CT and delayed contrast enhanced MRI. *Eur J Radiol.* 2012;81:2820-2825.

12. Moltz JH BL, Bornemann L, Kuhnigk JM, et al. Advanced segmentation techniques for lung nodules, liver metastases, and enlarged lymph nodes in CT scans. *J-STSP.* 2009;3:122-134.

13. Hellwig D, Graeter TP, Ukena D, et al. 18F-FDG PET for mediastinal staging of lung cancer: which SUV threshold makes sense? *J Nucl Med.* 2007;48:1761-1766.

14. Danielsen M, Hojgaard L, Kjaer A, Fischer BM. Positron emission tomography in the follow-up of cutaneous malignant melanoma patients: a systematic review. *Am J Nucl Med Mol Imaging.* 2013;4:17-28.

15. Kwekkeboom DJ, Kam BL, van Essen M, et al. Somatostatin-receptor-based imaging and therapy of gastroenteropancreatic neuroendocrine tumors. *Endocr Relat Cancer.* 2010;17:R53-R73.

16. Flechsig P, Choyke P, Kratochwil C, et al. Increased x-ray attenuation in malignant vs. benign mediastinal nodes in an orthotopic model of lung cancer. *Diagn Interv Radiol.* 2016;22:35-39.

17. Toloza EM, Harpole L, McCrory DC. Noninvasive staging of non-small cell lung cancer: a review of the current evidence. *Chest.* 2003;123:137S-146S.

18. Birim O, Kappetein AP, Stijnen T, Bogers AJ. Meta-analysis of positron emission tomographic and computed tomographic imaging in detecting mediastinal lymph node metastases in nonsmall cell lung cancer. *Ann Thorac Surg.* 2005;79:375-382.

19. Schaefer NG, Hany TF, Taverna C, et al. Non-Hodgkin lymphoma and Hodgkin disease: coregistered FDG PET and CT at staging and restaging--do we need contrast-enhanced CT? *Radiology.* 2004;232:823-829.

20. Gould MK, Kuschner WG, Rydzak CE, et al. Test performance of positron emission tomography and computed tomography for mediastinal staging in patients with non-small-cell lung cancer: a meta-analysis. *Ann Intern Med.* 2003;139:879-892.

21. Silvestri GA, Gould MK, Margolis ML, et al. Noninvasive staging of non-small cell lung cancer: ACCP evidenced-based clinical practice guidelines (2nd edition). *Chest.* 2007;132:178S-201S.

22. Beyer F, Buerke B, Gerss J, et al. Prediction of lymph node metastases in NSCLC. Three dimensional anatomical parameters do not substitute FDG-PET-CT. *Nuklearmedizin.*49:41-48; quiz N41.

23. Tournoy KG, Maddens S, Gosselin R, Van Maele G, van Meerbeeck JP, Kelles A. Integrated FDG-PET/CT does not make invasive staging of the intrathoracic lymph nodes in non-small cell lung cancer redundant: a prospective study. *Thorax.* 2007;62:696-701.

24. Miller AB, Hoogstraten B, Staquet M, Winkler A. Reporting results of cancer treatment. *Cancer.* 1981;47:207-214.

25. Therasse P, Arbuck SG, Eisenhauer EA, et al. New guidelines to evaluate the response to treatment in solid tumors. European Organization for Research and Treatment of Cancer, National Cancer Institute of the United States, National Cancer Institute of Canada. *J Natl Cancer Inst.* 2000;92:205-216.

26. Eisenhauer EA, Therasse P, Bogaerts J, et al. New response evaluation criteria in solid tumours: revised RECIST guideline (version 1.1). *Eur J Cancer.* 2009;45:228-247.

27. McIvor J, Siew T, Campbell A, McCarthy M. FDG PET in early stage cutaneous malignant melanoma. *J Med Imaging Radiat Oncol.* 2014;58:149-154; quiz 266.

28. Zattoni F, Guttilla A, Evangelista L. Can GA-PSMA or radiolabeled choline PET/CT guide salvage lymph node dissection in recurrent prostate cancer? *Eur J Nucl Med Mol Imaging.* 2016;43:1407-9.

29. Jensen TH, Bech M, Binderup T, et al. Imaging of metastatic lymph nodes by X-ray phase-contrast micro-tomography. *PLoS One.* 2013;8:e54047.

30. Puesken M, Buerke B, Gerss J, et al. Prediction of lymph node manifestations in malignant lymphoma: significant role of volumetric compared with established metric lymph node analysis in multislice computed tomography. *J Comput Assist Tomogr.* 2010;34:564-569.

31. Cuaron J, Dunphy M, Rimner A. Role of FDG-PET scans in staging, response assessment, and follow-up care for non-small cell lung cancer. *Front Oncol.*2:208.

32. Brown RS, Leung JY, Kison PV, Zasadny KR, Flint A, Wahl RL. Glucose transporters and FDG uptake in untreated primary human non-small cell lung cancer. *J Nucl Med.* 1999;40:556-565.

Figure 1: PET, CT- and PET/CT-images of PET+ and PET- LNs of patients with LC, MM, GEP-NET and PCA

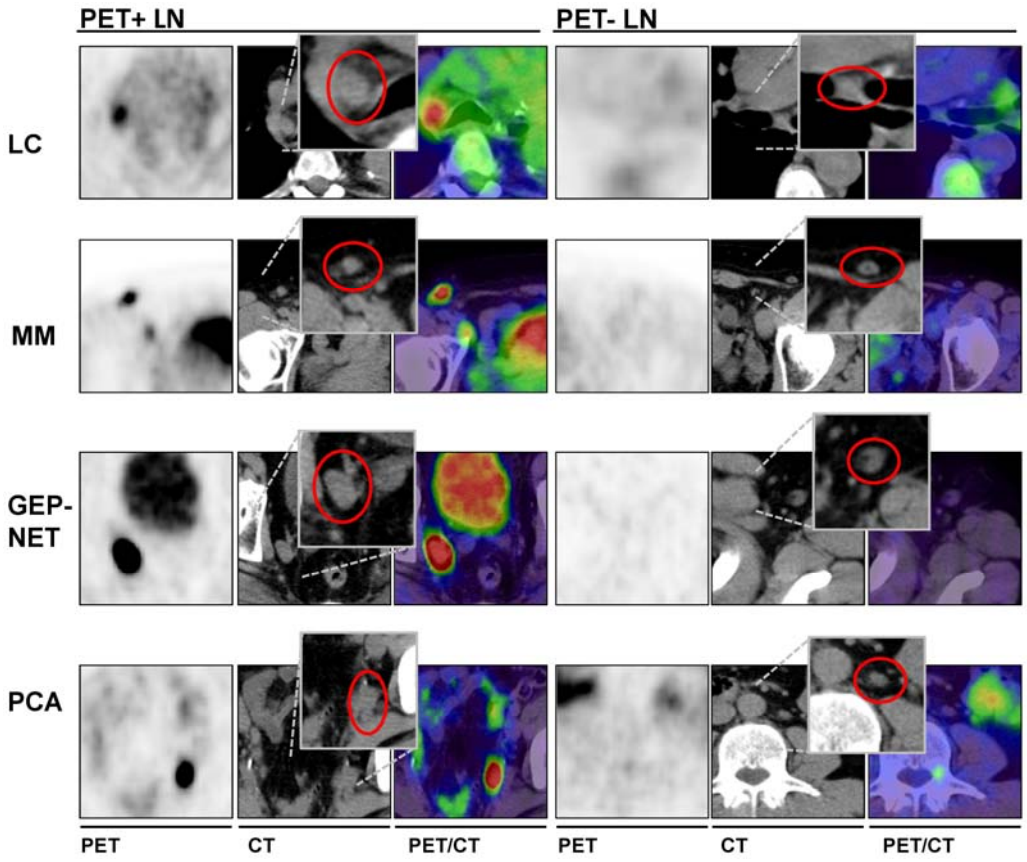

PET-image, native CT with magnified LN for density analysis, and fused PET/CT-image of LNs in patients with LC, MM, GEP-NET and PCA. Red circle in the magnified CT-image indicates the examined LN.

Figure 2: Statistical analysis of LNs in patients with LC

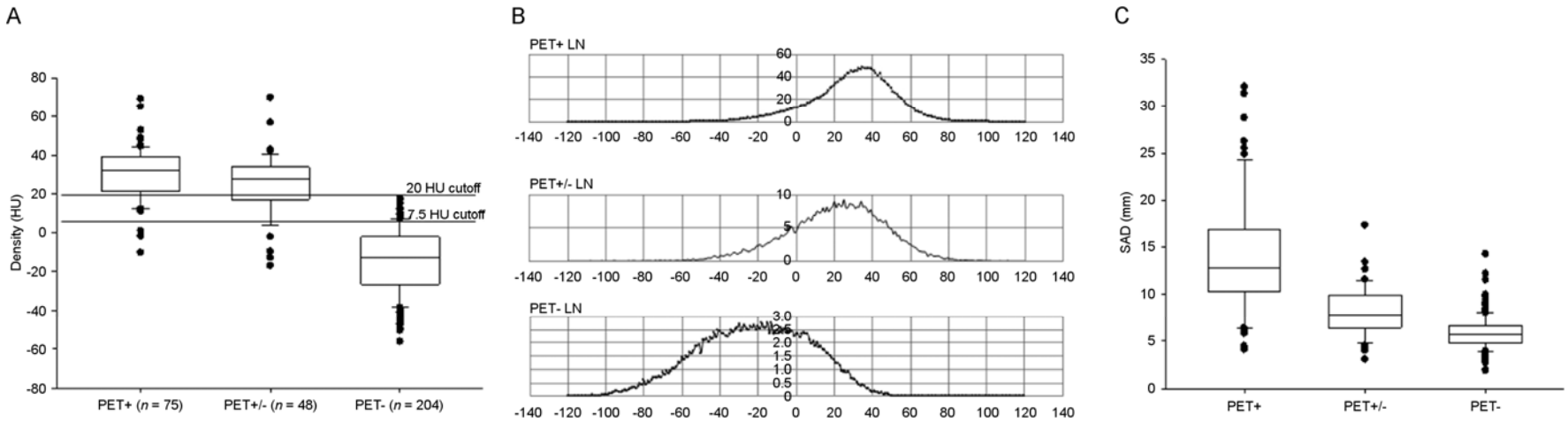

A) LN density in LC patients:
Box-plots with median and 95% confidence interval of PET+, PET+/- and PET- LNs in patients with LC. Cut off values with 7.5HU and 20 HU are illustrated as black lines. p-values for the statistical analysis between subgroups are demonstrated in Table 1.

B) LN histograms in LC patients:
Averaged histograms of PET+, PET+/- and PET- LNs in patients with LC.

C) SAD of LNs in patients with LC:
Boxplots with median, 25% and 75%-Quartiles of PET+, PET+/- and PET- LNs in patients with LC. p-values for the statistical analysis between subgroups are demonstrated in Table 1.

Figure 3: Statistical analysis of LNs in patients with MM

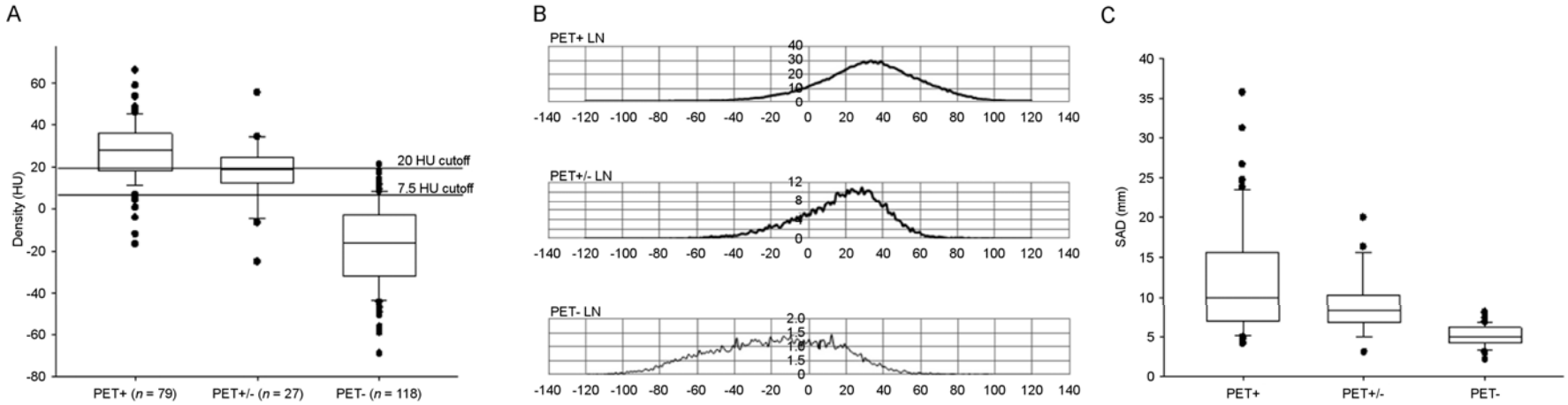

A) LN density in MM patients:
Box-plots with median and 95% confidence interval of PET+, PET+/- and PET- LNs in patients with MM. Cut off values with 7.5HU and 20 HU are illustrated as black lines. p-values for the statistical analysis between subgroups are demonstrated in Table 1.

B) LN histograms in MM patients:
Averaged histograms of PET+, PET+/- and PET- LNs in patients with MM.

C) SAD of LNs in patients with MM:
Boxplots with median, 25% and 75%-Quartiles of PET+, PET+/- and PET- LNs in patients with MM. p-values for the statistical analysis between subgroups are demonstrated in Table 1.

Figure 4: Statistical analysis of LNs in patients with GEP-NET

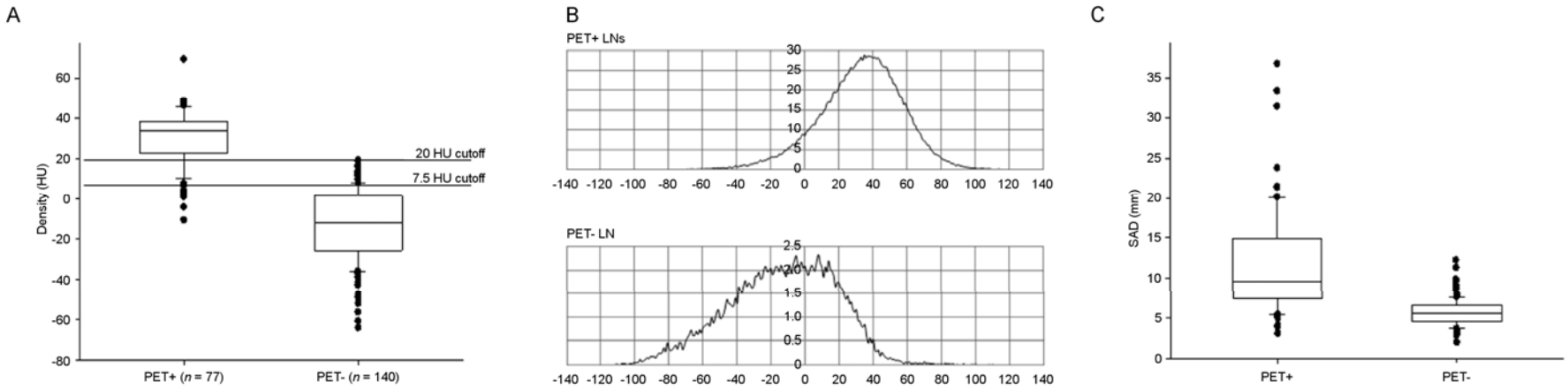

A) LN density in GEP-NET patients:
Box-plots with median and 95% confidence interval of PET+ and PET- LNs in patients with GEP-NETs. Cut off values with 7.5HU and 20 HU are illustrated as black lines. p-values for the statistical analysis between subgroups are demonstrated in Table 1.

B) LN histograms in GEP-NET patients:
Averaged histograms of PET+ and PET- LNs in patients with NET.

C) SAD of LNs in patients with GEP-NET:
Boxplots with median, 25% and 75%-Quartiles of PET+ and PET- LNs in patients with GEP-NET p-values for the statistical analysis between subgroups are demonstrated in Table 1.

Figure 5: Statistical analysis of LNs in patients with PCA

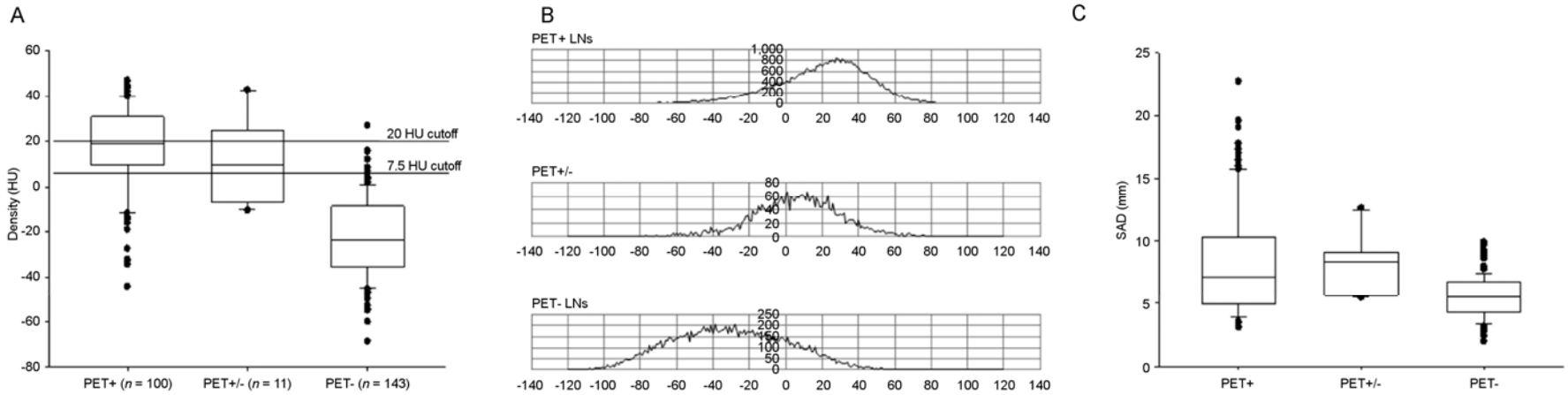

A) LN density in MM patients:
Box-plots with median and 95% confidence interval of PET+, PET+/- and PET- LNs in patients with PCA. Cut off values with 7.5HU and 20 HU are illustrated as black lines. p-values for the statistical analysis between subgroups are demonstrated in Table 1.

B) LN histograms in PCA patients:
Averaged histograms of PET+, PET+/- and PET- LNs in patients with PCA.

C) SAD of LNs in patients with MM:
Boxplots with median, 25% and 75%-Quartiles of PET+, PET+/- and PET- LNs in patients with PCA. p-values for the statistical analysis between subgroups are demonstrated in Table 1.

Figure 6: Density analysis of all LNs irrespective of tumour entity

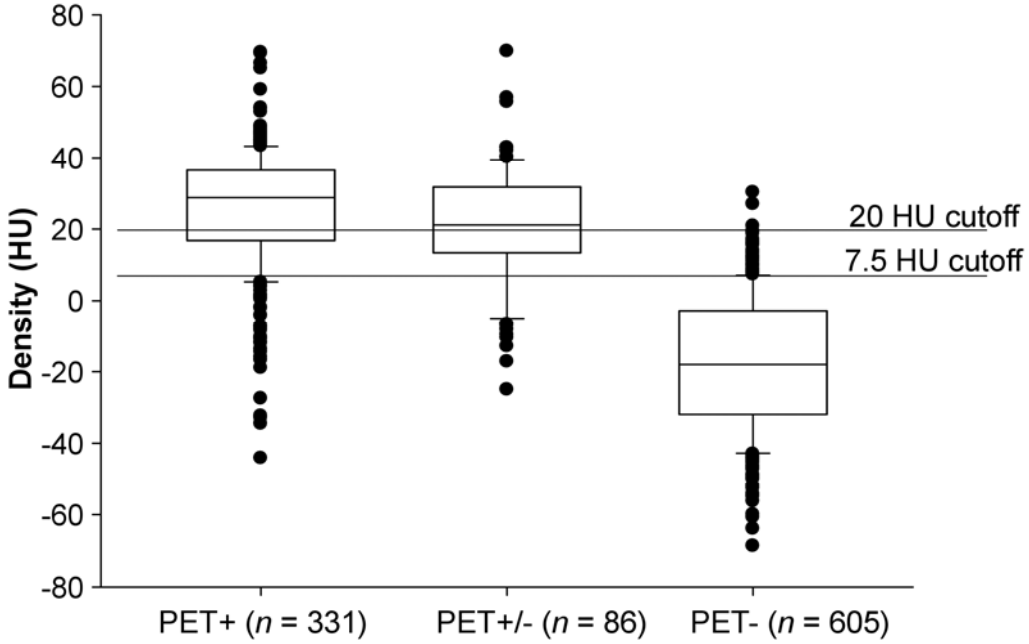

LN density:

Boxplots with median, 25% and 75%-Quartiles of PET+, PET +/- and PET- LNs in patients irrespective of tumour entity. Cut off values with 7.5HU and 20 HU are illustrated as black lines.

Table 1: correlation between PET- and CT-data

tumour entity		PET +	PET +/-	PET -	p (+ vs. +/-)	p (+ vs. -)	p (+/- vs. -)
LC	**LN (n)**	**75**	**48**	**204**			
	CT-density (HU)	31.3 (-10.4/39.2)	27.6 (-17.2/69.8)	-12.57 (-56.3/17.9)	0.08	<0.01	<0.05
	SAD (mm)	12.7 (4.1/32.1)	7.8 (3.1/17.3)	5.7 (1.9/14.2)	<0.01	<0.01	0.12
MM	**LN (n)**	**79**	**27**	**118**			
	CT-density (HU)	27.9 (-16.7/66.4)	19.1 (-15/55.7)	-16.3 (-69/21.2)	0.13	<0.01	<0.01
	SAD (mm)	10 (4.1/35.8)	8.3 (3.1/20)	5 (2.1/8.1)	<0.05	<0.01	<0.01
GEP-NET	**LN (n)**	**77**	**0**	**140**			
	CT-density (HU)	33.7 (-10.6/69.5)	-	-11.6 (-64/19.4)	-	<0.01	-
	SAD (mm)	9.7 (3.1/36.8)	-	5.6 (2/12.3)	-	<0.01	-
PCA	**LN (n)**	**100**	**11**	**143**			
	CT-density (HU)	19.2 (-44.2/47.1)	9.9 (-10.6/42.9)	-23.7 (-68.8/27)	0.06	<0.01	<0.05
	SAD (mm)	7.1 (3.1/22.7)	8.3 (5.5/12.6)	5.5 (1.9/9.9)	0.78	<0.01	0.21

Number (*n*) of LNs according to PET-status; CT-density (HU) and SAD (mm) with (minimum / maximum). *P*-values for two-sided t-test between different subgroups: exact p-value in cases of $p>0.05$; $p<0.05$ when $0.01<p<0.05$; $p<0.01$ when $p<0.01$.